of $SiHe^{n+}$ ions which display the strongest Si-He bonds and the greatest kinetic stability.

(2) In spite of the availability of extremely exothermic fragmentation processes, both the $SiHe^{3+}$ trication and $SiHe^{4+}$ tetracation are predicted to be potentially accessible species in the gas phase.

(3) The trends in the Si-He bond lengths in the series $SiHe^{n+}$ can readily be rationalized in terms of the number of electrons occupying the 5σ-antibonding molecular orbital.

(4) $SiHe^{4+}$, with just two valence electrons, is the smallest stable polyatomic tetracation yet reported in the literature.

Acknowledgment. We thank Peter Gill and Dr. Ross Nobes for helpful and stimulating discussions and Dr. Gernot Frenking for a preprint of ref 1c.

Registry No. $SiHe^{3+}$, 113161-95-8; $SiHe^{4+}$, 113161-96-9; Si, 7440-21-3; He, 7440-59-7.

Determination of ^{15}N Chemical Shift Tensor via ^{15}N-^{2}H Dipolar Coupling in Boc-glycylglycyl[^{15}N]glycine Benzyl Ester

Yukio Hiyama,[†,∥] Chien-Hua Niu,[§] James V. Silverton,[‡] Alfonso Bavoso,[‡,⊥] and Dennis A. Torchia*[†]

Contribution from the Bone Research Branch, National Institute of Dental Research, Laboratory of Chemistry, National Heart, Lung, and Blood Institute, and Laboratory of Experimental Carcinogenesis, National Cancer Institute, National Institutes of Health, Bethesda, Maryland 20892. *Received May 28, 1987*

Abstract: Proton-decoupled ^{15}N nuclear magnetic resonance line shapes of two crystalline phases of Boc-glycylglycyl[^{15}N,^{2}H]glycine benzyl ester are reported. Analysis of the spectra shows that ^{15}N-^{2}H bond distances are 1.042 and 1.050 Å, respectively, in the two phases and that the z axes of the chemical shift tensors make angles of 22° and 24° with respect to the N-H bond axis in each phase. In one phase the shift anisotropy is 168 ppm, and the asymmetry parameter has a small value, $\eta = 0.064$, typical of a peptide nitrogen. In contrast, an unusually large value of η, 0.44, is observed in the other phase of the peptide. Measurements of ^{15}N and ^{2}H relaxation times show that the difference in η values does not arise from molecular motion while measurements of ^{2}H quadrupole coupling constants indicate that hydrogen bond geometry is nearly the same in the two phases. X-ray diffraction shows that the phase having $\eta = 0.44$ has a triclinic lattice (a = 6.107 (3), b = 9.145 (4), c = 18.832 (2) Å; α = 76.36 (2), β = 85.42 (2), γ = 75.62 (4)°), while the phase having $\eta = 0.064$ has a monoclinic lattice (a = 13.228 (1), b = 9.259 (1), c = 17.118 (1) Å; β = 102.15 (1)°). Although only the monoclinic crystals were suitable for a complete structure determination, these differences in lattice and unit cell dimensions strongly suggest that the peptide assumes different conformations in the two phases. We discuss the possibility that a nonplanar peptide is the cause of the large asymmetry observed in the triclinic phase.

Solid-state ^{15}N NMR (nuclear magnetic resonance) spectroscopy has proven to be a useful tool for investigating the structure of fibrous proteins, where X-ray crystallography provides incomplete structural information.[1] The NMR studies, however, require thorough knowledge of the nitrogen chemical shift tensor: principal elements and their orientations. The orientation of the z principal axis of the ^{15}N chemical shift tensor of the peptide nitrogen in a single crystal of glycylglycine hydrochloride monohydride has been determined.[2] However, the minor principal axes' orientations were not determined[2] because of the commonly observed small asymmetry parameter (less than 0.1).

Herein, we report the orientations of ^{15}N chemical shift tensors in two crystalline forms of Boc-glycylglycyl[^{15}N,^{2}H]glycine benzyl ester. The shift tensor orientations were determined relative to the ^{15}N-^{2}H bond axis by analysis of proton-decoupled ^{15}N powder line shapes. In addition, we report values of ^{15}N-^{2}H bond distances, also obtained from the line shape analysis, and hydrogen bond distances obtained from measurements of ^{2}H quadrupole coupling constants.

A surprising observation was the large value of the asymmetry parameter ($\eta = 0.44$) obtained for one crystalline phase of the peptide. This large asymmetry is atypical of peptide nitrogen shift tensors, which normally have $\eta \leq 0.1$, as was found for the other crystalline form of $Boc(Gly)_3OBz$. X-ray diffraction showed that the peptide having $\eta = 0.44$ has a triclinic lattice while the η = 0.064 crystals have a monoclinic lattice. Although only the monoclinic crystals were suitable for a complete structure determination, unit cell parameters were determined for both crystalline forms and suggested that the difference in η resulted from differences in peptide conformations. In agreement with this conclusion, NMR relaxation measurements show that the differences in η do not arise from differences in molecular motion in the crystalline phases. We discuss possible conformational characteristics that could give rise to the large chemical shift asymmetry observed in the triclinic phase.

Experimental Section

$Boc(Gly)_3OBz$ was synthesized in the manner reported previously.[3] The triclinic phase of the peptide was recrystallized within 1 min by blowing nitrogen gas from a saturated dry (Na_2SO_4 anhydrous) ethyl acetate solution. The monoclinic phase was obtained from any one of the following solutions: wet ethyl acetate, chloroform, ethanol, or dry ethyl acetate with slow recrystallization. N-Deuteriated triclinic crystals were prepared by exchange in ethyl acetate/D_2O. Deuteriated monoclinic crystals were prepared by exchange in EtOD and were found to

[†] National Institute of Dental Research.
[‡] National Heart, Lung, and Blood Institute.
[§] National Cancer Institute.
[∥] Permanent address: Upjohn Pharmaceuticals Ltd., Nishi Shinjuku, Tokyo 160, Japan.
[⊥] Permanent address: Universita di Napoli, Dipartmento di Chemica, Via Mezzocannone 4, 80134, Naples, Italy.

(1) Cross, T. A.; Opella, S. J. *J. Mol. Biol.* **1985**, *182*, 367-381.
(2) Harbison, G. S.; Jelinski, L. W.; Stark, R. E.; Torchia, D. A.; Herzfeld, J.; Griffin, R. G. *J. Magn. Reson.* **1984**, *60*, 79-82.
(3) Niu, C.-H.; Black, S. *J. Biol. Chem.* **1979**, *254*, 265-267.

0002-7863/88/1510-2378$01.50/0

Table I. Positional and Equivalent Isotropic Temperature Factors for Heavier Atoms[a]

atom	x	y	z	U(equiv)
C4B	1944 (4)	4849 (6)	6966 (2)	905 (14)
C6B	1410 (3)	5272 (4)	8264 (2)	809 (12)
C5B	831 (3)	3022 (5)	7494 (3)	825 (12)
C3B	1681 (2)	4145 (3)	7696 (1)	553 (7)
C1B	3110 (2)	2413 (2)	7901 (1)	411 (5)
O2B	2606 (1)	3485 (2)	8186 (1)	456 (4)
O1B	2860 (1)	1892 (2)	7230 (1)	507 (5)
N1	3920 (1)	1970 (2)	8453 (1)	440 (5)
Cα1	4621 (2)	919 (2)	8244 (1)	452 (6)
C'1	5115 (2)	1502 (2)	7584 (1)	379 (5)
O1	5408 (1)	2762 (2)	7584 (1)	547 (5)
N2	5187 (1)	579 (2)	6997 (1)	378 (5)
Cα2	5505 (2)	1047 (2)	6283 (1)	424 (6)
C'2	4635 (2)	1550 (2)	5614 (1)	388 (5)
O2	4810 (1)	1749 (2)	4944 (1)	499 (5)
N3	3706 (1)	1742 (2)	5789 (1)	447 (5)
Cα3	2837 (2)	2236 (3)	5211 (1)	480 (7)
C'3	2923 (2)	3860 (3)	5033 (1)	601 (8)
O3	3617 (2)	4592 (2)	5303 (2)	831 (8)
O1*	2082 (2)	4263 (2)	4508 (1)	814 (8)
C1*	2129 (4)	5799 (4)	4263 (2)	976 (15)
C2*	1794 3)	6820 (3)	4863 (2)	821 (11)
C3*	2498 (3)	7652 (4)	5387 (3)	945 (14)
C4*	2159 (3)	8603 (4)	5908 (3)	947 (15)
C5*	1142 (4)	8682 (5)	5910 (3)	1127 (18)
C6*	465 (4)	7836 (6)	5406 (4)	1173 (20)
C7*	772 (3)	6920 (5)	4892 (3)	1011 (16)

[a] All parameters are multiplied by 10000. The equivalent U values are the geometric means of the diagonal terms of the vibration tensors. The trailing digit in an atom name indicates the residue number, e.g. "Cα1" is the α-carbon for residue 1. The asterisk indicates the O-benzyl protecting group and "B" the *tert*-butyl protecting group.

be ca. 80% deuteriated by ^1H NMR.

Equidimensional crystals obtained from a solution of chloroform had space group $P2_1/c$ and cell dimensions a = 13.228 (1) Å, b = 9.259 (1) Å, c = 17.118 (1) Å, β = 102.15 (1)°. The cell dimensions were measured with Cu Kα X-radiation (λ 1.5418 Å) and least-squares refinement of 20 reflections measured at ±θ in the θ range 20–25°. X-ray intensity data were collected with an Enraf-Nonius CAD4 diffractometer with monochromated Cu Kα radiation: crystal size 0.2 × 0.2 × 0.2 mm; θ(max) 74°; (sin θ)/λ(max) 0.6258 Å^{-1}; 4215 reflections having 3170 with $I > \sigma(I)$.

The phase problem was solved with MULTAN,[4] and refinement was by full-matrix least squares with isotropic thermal parameters for the H atoms and anisotropic parameters for the C, N, and O atoms. The anisotropic thermal parameters were of the form $\exp[-(2\pi^2(\sum_i\sum_j (U_{ij}h_ih_ja_i^*a_j^*)))]$. Weights were $1/\sigma$ with σ calculated as suggested by Peterson and Levy.[5] It proved expedient to hold the O-benzyl H atom thermal parameters at calculated values, but all other parameters were refined. The refinement converged at an R factor of 0.054, based on the 3170 "observed" reflections. Programs used for refinement were from XRAY[6] and, for the final reported results, XTAL.[7] A short table of atomic parameters for the heavier atoms is given as Table I, and a full list is available as supplementary material together with observed and calculated structure factors. A table of molecular dimensions is given as Table II.

Proton cross-polarized ^{15}N NMR spectra were obtained by a home-built double-resonance spectrometer with a Nicolet 1280 computer, operating at 250.45 MHz for proton.[9] The ^1H–^{15}N double-resonance probe contains a 5-mm-i.d., 10-mm-length solenoid coil. The 90° pulse was about 5 μs, and proton decoupling power was 50 kHz. The free induction decay was accumulated by a Nicolet 2090 Explorer scope with a dwell time of 10 μs. Spin–lattice relaxation time (T_1) and T_1 in the rotating frame ($T_{1\rho}$) of the proton and nitrogen-15 spins were measured through the proton-enhanced nitrogen-15 signal.[10] Proton cross-polarized ^{15}N

Table II. Molecular Dimensions for the Heavier Atoms[a]

C4B–C3B	1.514 (5)	C6B–C3B	1.520 (4)
C5B–C3B	1.517 (4)	C3B–O2B	1.464 (2)
C1B–O2B	1.343 (2)	C1B–O1B	1.225 (2)
C1B–N1	1.335 (2)	N1–Cα1	1.440 (3)
Cα1–C'1	1.519 (3)	C'1–O1	1.229 (2)
C'1–N2	1.337 (2)	N2–Cα2	1.441 (2)
Cα2–C'2	1.515 (2)	C'2–O2	1.230 (2)
C'2–N3	1.338 (2)	N3–Cα3	1.426 (2)
Cα3–C'3	1.543 (3)	C'3–O3	1.157 (3)
C'3–O1*	1.328 (2)	O1*–C1*	1.487 (4)
C1*–C2*	1.528 (5)	C2*–C3*	1.383 (5)
C2*–C7*	1.366 (5)	C3*–C4*	1.394 (6)
C4*–C5*	1.348 (6)	C5*–C6*	1.354 (6)
C6*–C7*	1.345 (7)		
C4B–C3B–C6B	111.0 (2)	C4B–C3B–C5B	113.3 (2)
C4B–C3B–O2B	110.0 (2)	C6B–C3B–C5B	110.7 (2)
C6B–C3B–O2B	101.6 (1)	C5B–C3B–O2B	109.5 (2)
O2B–C1B–O1B	125.1 (1)	O2B–C1B–N1	110.8 (1)
O1B–C1B–N1	124.1 (1)	C3B–O2B–C1B	121.3 (1)
C1B–N1–Cα1	119.6 (1)	N1–Cα1–C'1	110.2 (1)
Cα1–C'1–O1	121.4 (1)	Cα1–C'1–N2	116.2 (1)
O1–C'1–N2	122.3 (1)	C'1–N2–Cα2	121.6 (1)
N2–Cα2–C'2	115.0 (1)	Cα2–C'2–O2	119.3 (1)
Cα2–C'2–N3	117.3 (1)	O2–C'2–N3	123.4 (1)
C'2–N3–Cα3	122.1 (1)	N3–Cα3–C'3	111.6 (1)
Cα3–C'3–O3	125.2 (2)	Cα3–C'3–O1*	108.7 (2)
O3–C'3–O1*	126.0 (2)	C'3–O1*–C1*	112.4 (2)
O1*–C1*–C2*	111.5 (3)	C1*–C2*–C3*	122.0 (3)
C1*–C2*–C7*	119.7 (3)	C3*–C2*–C7*	118.3 (3)
C2*–C3*–C4*	120.3 (3)	C3*–C4*–C5*	119.4 (3)
C4*–C5*–C6*	119.6 (4)	C5*–C6*–C7*	122.1 (4)
C2*–C7*–C6*	120.3 (3)		

[a] The labeling follows Table I. Bond lengths are in angstroms and angles in degrees.

Table III. Torsion Angles of Boc(Gly)$_3$OBz

	φ	ψ	ω
Gly-1	60.7 (2)	−137.1 (2)	−174.2 (2)
Gly-2	−89.0 (2)	10.9 (3)	171.2 (2)
Gly-3	−77.8 (2)	−178.4 (2)	178.9 (4)

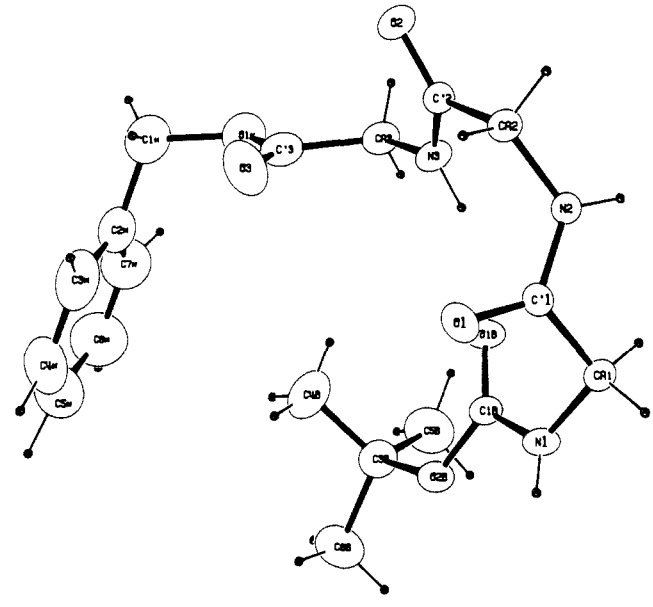

Figure 1. ORTEP[8] drawing showing the crystal conformation of Boc-(Gly)$_3$OBz in the monoclinic crystal. In the absence of Greek letters in the ORTEP font, the symbol "A" is used to indicate an α-carbon atom.

(4) Main, P.; Hull, S. E.; Lessinger, L.; Germain, G.; Declerq, J. P.; Woolfson, M. M. MULTAN 78, **1978**. A system of computer programs for the automatic solution of crystal structures from X-ray diffraction data, Universities of York, England, and Louvain, Belgium.

(5) Peterson, S. W.; Levy, H. A. *Acta Crystallogr.* **1957**, *10*, 70–75.

(6) Stewart, J. M.; Kruger, G. J.; Ammon, H. L.; Dickinson, C.; Hall, S. R. XRAY72, Technical Report No. TR-192; Computer Center, University of Maryland: College Park, MD, 1972.

(7) Stewart, J. M.; Hall, S. R.; Alden, R. A.; Olthof-Hazecamp, R.; Doherty, R. M. The XTAL system of crystallographic programs, 2nd ed., Technical Report No. TR-1364.1; University of Maryland: College Park, MD, March 1985.

(8) Johnson, C. K. ORTEP, Technical Report No. OR-3794; Oak Ridge National Laboratory: Oak Ridge, TN, 1965.

(9) Sarkar, S. K.; Sullivan, C. E.; Torchia, D. A. *J. Biol. Chem.* **1983**, *258*, 9762–9767.

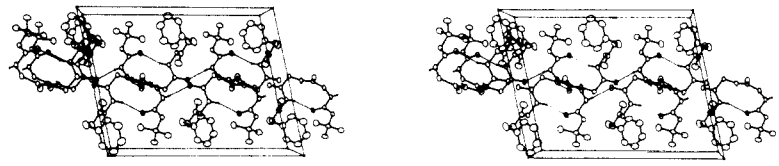

Figure 2. Molecular packing and hydrogen bonds of the monoclinic crystalline $Boc(Gly)_3OBz$. The direction of projection is b.

Table IV. Hydrogen Bond Dimensions

donor (D)	acceptor (A)	D···A, Å	H···A, Å	D–H···A, deg	symmetry operation
N1	O2	2.835 (2)	2.09 (2)	169 (2)	$x, {}^1/_2 - y, {}^1/_2 + z$ (glide)
N3	O1B	2.919 (2)	2.10 (3)	157 (2)	x, y, z (identity)
N2	O1	2.859 (2)	1.99 (3)	164 (2)	$1 - x, y - {}^1/_2, 1.5 - z$ (2_1)

magic-angle sample-spinning spectra were obtained by a Doty Scientific 5-mm probe. ^2H NMR spectra (38.45 MHz) were obtained by the same spectrometer with a single-tuned probe. The 90° pulse for the deuterium was 2 μs. ^2H spectra (76.76 MHz) were obtained by a NIC 500 with a 2090 Explorer scope.[11] The 90° pulse was 2.5 μs. Sampling time for all ^2H experiments was 500 ns.

Results

Crystalline Phases and X-ray Structure of $Boc(Gly)_3OBz$. The crystal conformation of the monoclinic crystal is shown in Figure 1, and bond lengths and angles are given in Table II. Geometrical parameters of the Boc and amide groups are in agreement with the literature data.[12,13] The Boc group has the "β" conformation with trans O1–C5 and trans C5–N1 bonds.[13] The values of the torsion angles are given in Table III. The torsion angles indicate that the Gly-1 residue has the D configuration. The overall pattern of conformational angles is consistent with a 4 → 1 trans (II) turn. The conformation is stabilized by an intramolecular hydrogen bond between the O atom of the urethane group and the H atom on the nitrogen of Gly-3 residue (N3···O distance 2.919 Å). The mode of packing of the structure is illustrated in Figure 2. A hydrogen bond (N···O distance 2.859 Å) between the N–H of amide 2 and the C=O of the amide 1 of a molecule related by the screw axis holds the structure along b. A hydrogen bond between the N–H of the urethane group and the C=O of the amide 2 of another molecule (N···O distance 2.835 Å) related by a glide plane holds the structure along the c direction (Table IV). The molecules interact through van der Waals forces between the hydrophobic *tert*-butyl and benzyl in the a direction. The overall packing may be described as hydrogen-bonded infinite sheets extended along the b and c axes and separated by hydrophobic groups on either side of the sheets. The nominal thermal parameters (Table I) indicate that large-amplitude molecular motions are absent in the crystal.

Cell dimensions, identical with those of crystals obtained from chloroform, were measured for crystals derived from ethanol and by slow (ca. 1 h) crystallization from dry ethyl acetate. However, rapid crystallization from the latter solvent yielded only microcrystals whose small size (largest dimension less than 100 μm) precluded an X-ray structure determination. The unit cell dimensions of the microcrystals were quite different from those of crystals obtained from chloroform and correspond to a triclinic cell (a = 6.107 (3), b = 9.145 (4), c = 18.832 (2) Å; α = 76.36 (2), β = 85.42 (2), γ = 75.62 (4)°). This result shows that the microcrystals of $Boc(Gly)_3OBz$, obtained from ethyl acetate, and the crystals, obtained from chloroform, have different three-dimensional structures and presumably different conformations.

^{15}N–^1H Double Resonance. The proton-enhanced and -decoupled ^{15}N spectra of the crystalline (monoclinic phase; Figure 3a) and microcrystalline (triclinic phase; Figure 3b) phases of Boc-Gly-Gly-[^{15}N]Gly-OBz have significantly different line shapes. Of particular interest is the unusually large asymmetry parameter, η = 0.44, observed in the spectrum of the microcrystalline sample. In contrast, the crystalline sample has a small asymmetry parameter, η = 0.064, typical of amide and peptide nitrogen asymmetry parameters reported previously.

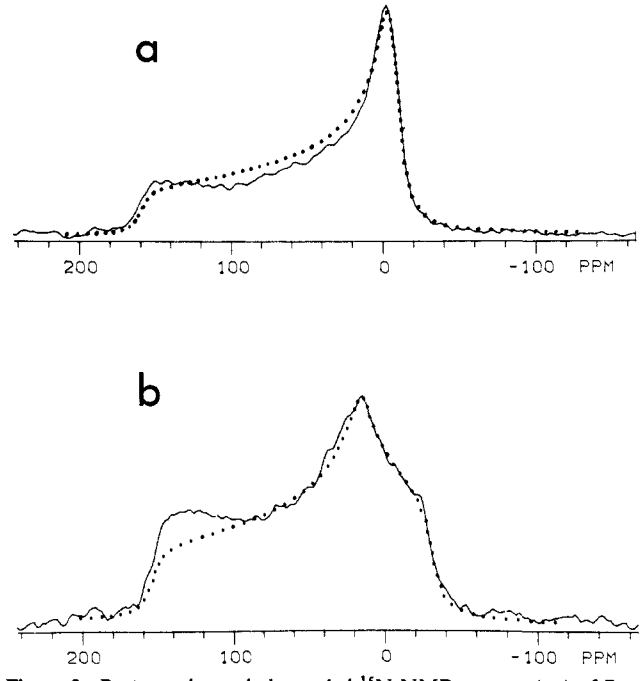

Figure 3. Proton enhanced-decoupled ^{15}N NMR spectra (—) of Boc-Gly-Gly-[^{15}N]Gly-OBz: (a) crystalline phase (monoclinic), (b) microcrystalline phase (triclinic). Conditions: 1-ms contact, 2-s repetition time, 100-Hz Lorentzian broadening applied. Theoretical spectra (···) were calculated with the chemical shift tensor elements listed in Table V. The theoretical line shapes in (a) and (b) were convoluted with Lorentzian line shapes having widths 250 and 300 Hz, respectively. Chemical shift scale relative to carrier frequency.

Our measurements of large ^{15}N T_1 (≃120 s) and $T_{1\rho}$ (≫10 ms) values showed that molecular motion at the nitrogen site was negligible and was therefore not the source of the difference in line shapes observed in Figure 3.

Because the ^{15}N T_1 value is so large, whereas the ^1H T_1 value is small (ca 0.4 s, presumably because of methyl reorientation in the Boc moiety), ^{15}N spectra were obtained by a Hartmann–Hahn matched cross-polarization pulse sequence. The effect of contact time upon the shapes of the powder patterns was monitored by obtaining a series of spectra as a function of the contact time. It was found, with optimal Hartmann–Hahn matching, that the three principal directions in the powder pattern attained full intensity with a contact time of 300 μs and that all components of the spectrum attained nearly full intensity with a contact time of 1 ms. Because this contact time is much less than the $T_{1\rho}$ of either the protons (ca. 10 ms) or the ^{15}N (>10 ms), the observed spectra should closely represent those of the ^{15}N chemical shift powder line shapes in the two crystalline phases of Boc-Gly-Gly-[^{15}N]-Gly-OBz. Computer-generated line shapes (dotted curves in Figure 5a,b) calculated with the parameters listed in Table V do show some departures from the observed line shapes. This observation is a consequence of inefficient polarization transfer for spectral components that correspond to near magic-angle orientations of the ^1H–^{15}N bond with respect to the external field.

(10) Torchia, D. A. *J. Magn. Reson.* **1978**, *30*, 613–616.
(11) Hiyama, Y.; Silverton, J. V.; Torchia, D. A.; Gerig, J. T.; Hammond, S. J. *J. Am. Chem. Soc.* **1986**, *108*, 2715–2723.
(12) Benedetti, E. Proceedings of the Fifth American Peptide Symposium, 1977; pp 257–273.
(13) Benedetti, E.; Pedone, C.; Toniolo, C.; Nemethy, G.; Pottle, M. S.; Scheraga, H. A. *Int. J. Pept. Protein Res.* **1980**, *16*, 156–172.

Table V. Chemical Shift Anisotropy of Nitrogen-15 in Boc-Gly-Gly-[^{15}N]Gly-OBz[a]

	σ_{11}	σ_{22}	σ_{33}	σ_{iso}	σ_{xx}	σ_{yy}	σ_{zz}	η
monoclinic	157.2	318.1	325.1	58.3	58.3 (−1479,	51.3 1301,	109.6 2781)	0.064
triclinic	159.8	296.8	343.8	266.8	77.0 (−1954,	30.0 761,	−107.0 2715)	0.440

[a] σ_{ii} (i = 1–3) are relative to external neat CH_3NO_2. $\sigma_{33} \geq \sigma_{22} \geq \sigma_{11}$. $\sigma_{iso} = {}^1/_3(\sigma_{11} + \sigma_{22} + \sigma_{33})$. $|\sigma_{zz}| \geq |\sigma_{xx}| \geq |\sigma_{yy}|$; $\sigma_{xx} + \sigma_{yy} + \sigma_{zz} = 0$; and $\eta = (\sigma_{yy} - \sigma_{xx})/\sigma_{zz}$. The isotropic shifts, σ_{iso}, of both crystalline and microcrystalline phases are essentially identical with that in chloroform solution that is 73 ppm downfield from glycine in 0.01 N HCl. Values in parentheses are σ_{xx}, σ_{yy}, and σ_{zz} in hertz at 25.38 MHz.

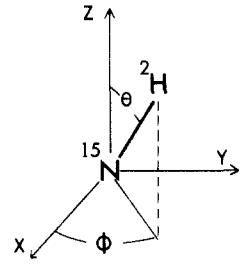

Figure 4. ^{15}N–^2H bond axis—the Z principal axis of the dipolar tensor—in principal-axis system of nitrogen-15 chemical shift tensor (σ_{xx}, σ_{yy}, σ_{zz}) ($|\sigma_{zz}| \geq |\sigma_{xx}| \geq |\sigma_{yy}|$).

However, the line shape discrepancies do not interfere with accurate determination of the shift tensor principal frequencies, and these quantities are the essential information contained in the powder spectrum. The principal shielding components derived from the powder patterns are listed in Table V. Despite the large difference in the asymmetry parameters, magic-angle sample-spinning ^{15}N NMR spectra of both the microcrystalline and crystalline phases showed an identical isotopic shift within 0.5 ppm. The isotropic chemical shifts in the solid phases were identical with that in chloroform solution within experimental error that is 73 ppm downfield from glycine in 0.01 N HCl, which is typical of the chemical shift observed for a glycyl residue in a peptide.[14]

Although single crystals large enough for NMR studies were not obtained for either crystalline phase of Boc(Gly)$_3$OBz, we were able to determine the orientation of the ^{15}N chemical shift tensor principal-axis system relative to the ^{15}N–H bond axis. This was accomplished by analysis of the ^{15}N powder line shape of each crystalline form of Boc-Gly-Gly-[^{15}N,^{2}H]Gly-OBz, in the following manner.

^{15}N–(^{2}H) Powder Spectra. A deuterium-coupled (proton-decoupled) ^{15}N NMR spectrum is a superposition of the powder line shapes corresponding to the three eigenstates of ^2H spin system, $|+1\rangle$, $|0\rangle$, and $|-1\rangle$. Three eigenvalues of these states, $m_s = +1$, 0, and −1, are good quantum numbers because the ^2H nuclear quadrupole interaction (e^2Qq_{zz}/h; ca. 200 kHz) is small compared to the Larmor frequency (38.45 MHz) and therefore causes only small mixing (0.5%) among the spin states. Likewise, because the size of the ^{15}N–^2H dipolar interaction ($\gamma(^{15}N)\cdot\gamma(^2H)/r^3 = 1.865/r^3$ kHz, where r is in angstroms) is much smaller than the ^{15}N Zeeman interaction (Larmor frequency 25.38 MHz), only the secular term A of the dipolar interaction need be considered.[15] As a consequence of these considerations, the principal frequencies of the ^{15}N powder line shape are determined by a tensor, $\tilde{\nu}$, given by

$$\tilde{\nu} = \tilde{C} + m_s\cdot\tilde{D} \qquad m_s = +1, 0, -1$$

where $\tilde{C}$ and $\tilde{D}$ are ^{15}N chemical shift tensor and ^{15}N–^2H dipolar coupling tensor, respectively. We write elements of the two tensors in the principal-axis system of the chemical shift tensor (Figure 4) where the chemical shift tensor is diagonal and is given by

$$\tilde{C} = C\begin{pmatrix} -{}^1/_2(1+\eta) & 0 & 0 \\ 0 & -{}^1/_2(1-\eta) & 0 \\ 0 & 0 & 1 \end{pmatrix}$$

(14) Martin, G. T.; Martin, M. L.; Gouesnard, J.-P. *NMR Basic Principles and Progress*: Springer: Berlin, 1981; Vol. 18.
(15) Slichter, C. P. *Principles of Magnetic Resonance*; Springer: Berlin, 1978; p 58.

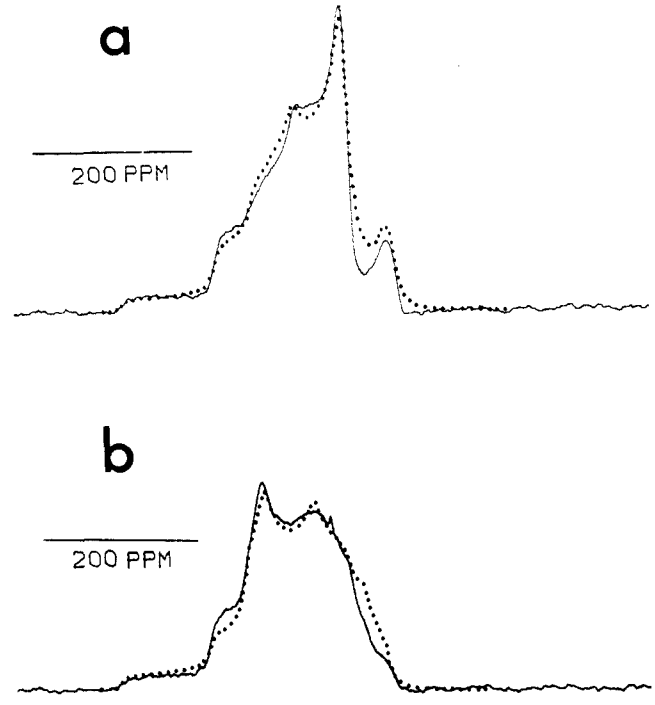

Figure 5. Observed proton enhanced-decoupled ^{15}N NMR spectra (—) of Boc-Gly-Gly-[^{15}N,^{2}H]Gly-OBz: (a) crystalline phase (monoclinic), (b) microcrystalline phase (triclinic). Contact time was 2 ms. Theoretical spectra (···) were obtained with the calculated principal frequencies listed in Table VI. The $m_s = 0$ component of (a) was given a relative weight of 1.8 in the calculations since this sample was 20% protonated. Calculated spectra were convoluted with Lorentzian line shapes having widths of 300 Hz.

with $C = \sigma_{zz}$. In the chemical shift principal-axis system, the dipolar tensor, $\tilde{D}$, is axially symmetric but not diagonal and is given by[16]

$$\tilde{D} = (D_{ij}) \qquad D_{ij} = D_{ji}$$

$$D_{xx} = D(-1 + 3\sin^2\Theta\cos^2\Phi)$$

$$D_{yy} = D(-1 + 3\sin^2\Theta\sin^2\Phi)$$

$$D_{zz} = D(3\cos^2\Theta - 1)$$

$$D_{xy} = -D/2(3\sin^2\Theta\sin^2\Phi)$$

$$D_{xz} = -D/2(3\sin 2\Theta\cos\Phi)$$

$$D_{yz} = D/2(3\cos 2\Theta\sin\Phi)$$

D is the ^{15}N–^2H dipolar coupling constant ($=\gamma(^{15}N)\cdot\gamma(^2H)/r^3$), and ($\Theta$, Φ) are polar angles of the N–H internuclear vector. Note that $|\sigma_{zz}| \geq |\sigma_{xx}| \geq |\sigma_{yy}|$ and $\eta = (\sigma_{yy} - \sigma_{xx})/\sigma_{zz}$.

The calculated values of the principal frequencies, ν_{11}, ν_{22}, and ν_{33}, for each multiplet ($m_s = +1$, 0, −1) of the powder line shape are obtained by diagonalizing ν. Figure 5 shows ^{15}N powder spectra of N-deuteriated (a) monoclinic (crystalline) and (b) triclinic (microcrystalline) Boc-Gly-Gly-[^{15}N,^{2}H]Gly-OBz. The experimental values of the principal frequencies of each multiplet

(16) Spiess, H. W. *NMR Basic Principles and Progress*; Springer: Berlin, 1978; Vol. 11.

Table VI. Principal Frequencies[a] of ^{2}H-Coupled ^{15}N Powder Pattern in Boc-Gly-Gly-[^{15}N,^{2}H]Gly-OBz

	$m_s = +1$			$m_s = -1$		
	ν_{t1}	ν_{22}	ν_{33}	ν_{11}	ν_{22}	ν_{33}
monoclinic						
exptl[b]	5680	−2684	−3018	1580	250	−1830
calcd[c]	5703	−2680	−3023	1604	250	−1854
triclinic						
exptl[b]	5685	−2535	−3150	1510	1040	−2538
calcd[c]	5600	−2410	−3190	1516	890	−2406

[a] In hertz. [b] Experimental values were obtained by fitting the observed spectra. [c] Calculated values were obtained with (Θ, Φ) = (22°, ---), D = 1.625 kHz, for the crystalline phase and (Θ, Φ) = (24°, 0°), D = 1.650 kHz, for the microcrystalline phase.

were determined by computer-fitting each line shape and are listed in Table VI. It is seen in Table VI that the $m_s = +1$ multiplets of both the monoclinic and triclinic phases have large anisotropies of nearly 9 kHz and small asymmetry parameters. On the other hand, the anisotropies of the $m_s = -1$ components of the line shapes are less than 4.1 kHz. In addition, the asymmetry parameters are drastically different in the two crystalline phases.

In order to calculate the powder spectrum for each multiplet, five parameters (C, D, η, Θ, Φ) are required. The values of C and η for the two crystalline phases were obtained from the corresponding proton-decoupled ^{15}N spectra (Figure 3; Table V). The dipolar coupling constant, D, was constrained to lie in the range from 1.4 to 1.9 kHz, because values of D outside this range corresponded to unreasonable internuclear N–D bond distances, i.e. outside the 1.0–1.1-Å range. The orientation of the N–D bond was varied over all directions by changing the polar angles (Θ, Φ) in 10° steps. When the $m_s = +1$ component of the crystalline and microcrystalline line shapes was analyzed, it was immediately clear that the angle Θ had to be less than 30° in order to reproduce the large value observed for ν_{11}. This result has the important implication that the σ_{zz} direction is nearly parallel to the N–D bond axis. In the case of the crystalline phase we observed frequencies for the $m_s = +1$ multiplet, with D ranging from 1.55 to 1.65 kHz and Θ ranging from 18.5° to 24.0°. In contrast with the $m_s = +1$ tensor elements, the off-diagonal elements of the ν tensor are important when $m_s = -1$ because the dipolar and chemical shift interactions cancel, making the diagonal terms small. This causes large shifts in the principal frequencies. In order to fit the observed principal frequencies of the $m_s = -1$ multiplet, Θ had to be 22 ± 1°, while D was in the range 1.55–1.70 kHz. When the $m_s = +1$ and $m_s = -1$ results were conbined, D and Θ were determined to be 1.6125 (±0.025) kHz and 22 (±1)° for the crystalline phase. We were not able to determine Φ because of the small asymmetry parameter of the ^{15}N chemical shift tensor. The value of the dipolar coupling corresponds to a ^{15}N–^{2}H internuclear distance of 1.050 (±0.006) Å in the crystalline phase.

In a similar fashion, the dipolar coupling constant D and polar angles (Θ, Φ) in the microcrystalline phase were determined to be 1.650 (±0.025) kHz and (24 (±1)°, 0 (±10)°), respectively. Note that Φ could be determined in the microcrystalline phase because of the large asymmetry parameter of the ^{15}N chemical shift tensor. The corresponding ^{15}N–^{2}H internuclear distance is 1.042 (±0.006) Å, which is slightly shorter than in the crystalline phase. The line shapes obtained using the calculated principal frequencies listed in Table VI are compared with the experimental line shapes in Figure 5. As expected on the basis of the results in Figure 3, the calculated and observed line shapes show some differences, but the principal frequencies derived from the observed and calculated spectra are in good agreement (Table VI).

Although our analysis of the microcrystalline line shape yields the orientation of the N–H bond in the chemical shift tensor principal-axis system (PAS), this information does not enable us to assign the principal axes of the ^{15}N chemical shift tensor in the molecular frame of the peptide bond. These assignments can be made if one assumes that the σ_{zz} ($=\sigma_{11}$) axis lies in the peptide plane and is nearly orthogonal to the N–C′ bond direction as found in the single-crystal ^{15}N NMR study of Gly-Gly-HCl monohydrate.[2] This assumption, together with the value of (Θ, Φ) obtained from the line shape simulation yields the unique CSA PAS orientation illustrated in Figure 6. Examination of Figure 6 shows that the σ_{xx} ($=\sigma_{33}$) direction is nearly parallel to the N–C′ bond axis and that σ_{yy} ($=\sigma_{22}$) is normal to the peptide plane. In the case of the crystalline sample the orientation of σ_{zz} is close to that shown in Figure 6; however, since $\eta \simeq 0$ the orientations of σ_{xx} and σ_{yy} are undetermined. A similar problem was encountered in the single-crystal NMR study of Gly-Gly-HCl monhydrate where the ^{15}N chemical shift tensor is nearly axially symmetric.

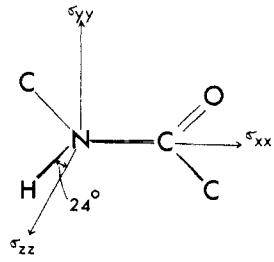

Figure 6. ^{15}N chemical shift tensor orientation in the peptide molecular frame of the microcrystalline phase (triclinic).

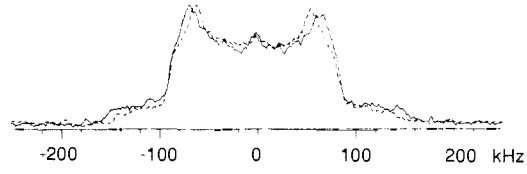

Figure 7. 76.76-MHz ^{2}H NMR spectra of amide deuterons in Boc-(Gly)$_3$OBz: (—) crystalline phase, (---) microcrystalline phase.

Table VII. ^{2}H Quadrupole Coupling Constants of Peptide Hydrogens in Boc(Gly)$_3$OBz

site	e^2Qq/h, kHz	η	N···O, Å NMR	N···O, Å X-ray	asignt
		Monoclinic Crystalline			
A	180	0.20	2.80	2.835	Gly 1
B	185	0.18	2.83	2.859	Gly 2
C	196	0.18	2.91	2.919	Gly 3
		Triclinic Crystalline[a]			
A′	192	0.15	2.88		
B′	209	0.14	3.00		
C′	211	0.13	3.01		

[a] No assignments can be made for the triclinic crystals because of no X-ray data.

Although the chemical shift tensors of the crystalline and microcrystalline samples have similar values of σ_{zz} and σ_{iso}, they have different values of σ_{yy} and σ_{xx}. This results in powder patterns having distinctly different line shapes as a consequence of their different asymmetry parameters.

In order to check whether the observed difference in η might arise from differences in hydrogen bonding in the two phases of the peptide, deuterium quadrupole coupling constants (which are sensitive to hydrogen bond geometry)[17] were derived from powder ^{2}H NMR spectra of Boc-[N,^{2}H]Gly-[N,^{2}H]Gly-[N,^{2}H]Gly-OBz (Figure 7). The ^{2}H quadrupole coupling constants and asymmetry parameters (Table VII) were determined by computer simulating the line shape with asymmetry parameters ranging from 14 to 20%. In the crystalline phase all quadrupole coupling constants were found to be less than 200 kHz. This result indicates that all nitrogen atoms are involved in strong (intra or inter) hydrogen bonds. The assignments listed in Table VII were made on the basis of the N–O distances obtained from the X-ray study and the empirical distance coupling constant relationship.[17] The nitrogen site of interest (N3) has deuterium quadrupolar param-

(17) (a) Soda, G.; Chiba, T. *J. Chem. Phys.* **1969**, *50*, 439–455. (b) Hunt, M. J.; Mackay, A. L. *J. Magn. Reson.* **1974**, *15*, 402–414. (c) Hiyama, Y.; Keiter, E. A.; Brown, T. L. *J. Magn. Reson.* **1986**, *67*, 202–210.

eters of e^2Qq_{zz}/h = 196 kHz and η = 0.18. Although the deuterium quadrupole coupling constants in the microcrystalline phase are larger, the corresponding N-O distances are only slightly longer than found in the crystalline phase (Table VII). In the site of particular interest (N3), the N···O hydrogen bond length in the microcrystalline phase is, at most, 0.1 Å greater than in the crystalline phase. Therefore, the difference in hydrogen bonding to the two phases is small and is unlikely to be the major source of the different ^{15}N chemical shift asymmetry parameters observed in the two phases. Spin-lattice relaxation times of the peptide deuterons in both the monoclinic and triclinic phases were about 15 s, suggesting that all the nitrogen sites are rigid in both crystalline phases.

Discussion

We have shown that a straightforward analysis of ^{15}N-^2H dipolar-coupled ^{15}N line shapes yields precise values of ^{15}N-^2H bond distances as well as the orientation of ^{15}N chemical shift tensor relative to the N-H bond axis (the z axis of the dipolar tensor). The proton-decoupled ^{15}N-^2H dipole-coupled ^{15}N spectra exhibit the ^{15}N-^2H coupling in a straightforward fashion and are simple to analyze because the coupled spins can be treated as an isolated two-spin system. The determination of bond distances from ^{15}N-^1H dipole-coupled ^{15}N spectra requires application of a more complex pulse sequence to eliminate homonuclear proton coupling. The decoupling sequence scales the ^{15}N-^1H coupling, thereby requiring the measurement of the scale factor in order to extract distance information from such spectra.[18] Although double labeling is required to observe the ^{15}N-^2H coupled spectrum, this is readily accomplished because the peptide hydrogen is exchangeable.

The internuclear ^{15}N-^2H bond distances obtained from the analysis of the NMR line shapes are 1.04-1.05 Å in the two crystalline forms of the peptide. These distances are 0.02-0.03 Å greater than typical peptide N-H bond distances obtained from neutron diffraction[19] but agree with bond distances obtained from another NMR study.[18]

Undoubtedly, the NMR and neutron studies yield different values of the N-H bond distance because molecular motions affect the outcome of the two types of experiments in different ways. In particular, librational motions of the ^{15}N-^2H bond reduce the magnitude of the ^{15}N-^2H dipole-dipole coupling. Because the observed (averaged) dipolar coupling is smaller than the static coupling, the value of the internuclear distance obtained from the analysis of the powder line shapes overestimates the bond length. In the case of $Boc(Gly)_3OBz$, the observed coupling yields ^{15}N-^2H bond lengths of 1.04-1.05 Å. However, the observed coupling yields a bond length of 1.02 Å if we assume that the ^{15}N-^2H bond axis undergoes restricted diffusion (rms angle 12-14°) in a cone. We therefore conclude that as a consequence of bond librations the distances obtained from the NMR likely overestimate the ^{15}N-^2H bond length by ca. 0.02 Å.

Because the librational frequencies are much greater than ω_0, these small-amplitude motions do not contribute significantly to spin-lattice relaxation in either the laboratory or rotating frame. Therefore, we observed large values of T_1 and $T_{1\rho}$ for ^{15}N and ^2H nuclei in both crystalline forms of the peptide.

The similarity in ^{15}N-^2H internuclear distances found in the two crystalline forms of the peptide contrasts with the large difference in ^{15}N shift tensor asymmetry parameters obtained in the two crystalline phases. The large differences in unit cell shapes and sizes in the two crystalline phases suggest that a difference in peptide conformation may account for the difference in η. Unfortunately, the unusually large value of η (0.44) was observed for the triclinic phase, which yielded microcrystals that were not suitable for an X-ray structure determination. The ^2H NMR spectra showed that this phase had normal hydrogen bond lengths, so that it is not likely that the large η value is caused by an unusual hydrogen bond. One intriguing possibility is that the large η results from a nonplanar peptide bond in the triclinic phase. Nonplanar peptide bonds have been reported in a number of peptide crystal structures.[20] The principal elements of the ^{15}N shift tensor should be very sensitive to the overlap of the carbonyl carbon and nitrogen π orbitals. To our knowledge, molecular orbital calculations of ^{15}N chemical shift tensor elements have not been carried out. In view of the importance of the peptide bond conformation in determining peptide and protein structure, we hope that this study stimulates further theoretical and experimental work to determine whether the asymmetry of the CSA tensor is correlated with the conformation of the peptide bond.[21]

Registry No. BOC-Gly-Gly-[^2H,^{15}N]Gly-OBzl, 113353-39-2.

Supplementary Material Available: Tables of positional and refined parameters and hydrogen atom parameters (2 pages); listing of observed and calculated structure factors (20 pages). Ordering information is given on any current masthead page.

(18) Roberts, J. E.; Harbison, G. S.; Munowitz, M. G.; Herzfeld, J.; Griffin, R. G. *J. Am. Chem. Soc.* **1987**, *109*, 4163-4169.
(19) Keiter, E. A. Ph.D. Thesis, University of Illinois, 1986.
(20) (a) Mauger, A. B.; Stuart, O. A.; Highet, R. J.; Silverton, J. V. *J. Am. Chem. Soc.* **1982**, *104*, 174-180. (b) Mauger, A. B.; Stuart, O. A.; Ferretti, J. A.; Silverton, J. V. *J. Am. Chem. Soc.* **1985**, *107*, 7154-7163.
(21) Ando, S.; Yamanobe, T.; Ando, I.; Shoji, A.; Ozaki, T.; Tabeta, R.; Saito, H. *J. Am. Chem. Soc.* **1985**, *107*, 7648-7652.

Head-Group Orientation of a Glycolipid Analogue from Deuterium NMR Data

Preetha Ram and J. H. Prestegard*

Contribution from the Chemistry Department, Yale University, New Haven, Connecticut 06511.
Received July 7, 1987

Abstract: A methodology is presented for the conformational analysis of glycolipid head groups in membrane-like environments. The methodology depends on orientational data, in the form of deuterium quadrupolar splittings, obtained in field-ordered liquid crystalline arrays of fatty acid micelles. The orientational data are incorporated into a molecular mechanics program in the form of a pseudoenergy term that minimizes when the molecular conformation satisfies orientational constraints. A minimum in a complete energy function, incorporating both theoretical and experimental constraints, is then sought. Using this approach it has been possible to predict a reasonable conformation for the sugar head group of (*N*-dodecyl)-4-*O*-β-D-galactopyranosyl-D-gluconylamide, a glycolipid analogue, anchored to a micelle surface.

Oligosaccharide moieties of membrane glycoproteins and glycolipids play important roles as receptors for hormones, bacterial toxins, viruses, and other agents which influence cellular function.[1,2] A knowledge of the conformational properties of these oligo-

0002-7863/88/1510-2383$01.50/0